

FORMULATION AND CHARACTERIZATION OF BETULINIC ACID LOADED POLYMERIC NANOPARTICLES FOR THE TREATMENT OF BREAST CANCER

Mr. Meghraj Vivekanand Suryawanshi¹, Dr. Hitendra S. Mahajan²

Department of Pharmaceutics, SES'S R.C.Patel Institute of Pharmaceutical Education and Research, Shirpur Maharashtra-425405

Abstract

The natural triterpenoid Betulinic acid has shown the anticancer properties. It showed poor aqueous solubility and high lipophilic nature. The aim of the study was to develop BA loaded Lycoat RS 720-BSA conjugated polymeric nanoparticles by the way of increasing solubility, bioavailability. Lycoat RS 720-BSA conjugate was prepared by Maillard Reaction. BA loaded nanoparticles was prepared by the solvent evaporation method. The detection of BA was determined by the HPLC at 210 nm. The nanoparticles showed spherical shape with particle size 257 nm. The formulation showed the zeta potential -22.4 mV. The optimized batch showed the entrapment efficiency 88.32% and drug loading 6.84%. The drug content of optimized batch was found to be 78.10%. The in-vitro diffusion study show sustained release pattern and % diffusion was found to be 94.24% after 24 hrs. The in-vitro anticancer activity and accelerated stability study was performed.

Keyword: Betulinic acid, Conjugation, Lycoat RS 720, Bovine Serum Albumin, Anticancer

1.INTRODUCTION

Nanoparticles can be defined as particulate dispersions or solid particles with a size in the range of 10-1000 nm [1]. They are mostly attractive for cancer treatment due to their small size, varied composition, surface functionalization, and stability which deliver exclusive opportunities to interact and target the tumor microenvironment [2, 3]. Nanoparticles are made from biocompatible and biodegradable polymers either natural or synthetic are called as polymeric nanoparticles. They have been inspected specially in

drug delivery and drug targeting owing to their particle size and long circulation in the blood [2, 3, and 4].

Cancer is the uncontrolled growth of abnormal cells. Cancer growths, when the body not works in normal mechanism. In malignancy condition, old cells don't die and formed new abnormal cells. These extra cells may form a mass of tissue, called tumor. Breast cancer mentions to cancers originating from breast tissue, mostly from the inner lining of milk ducts or the lobules that supply the ducts with milk. Currently, breast cancer is the most regularly detected life-threatening cancer in women and the foremost cause of cancer death among women [5]. Breast cancer is the most common cause of cancer in women and the second most common cause of cancer death in women in the United States. Universally, breast cancer comprises 10.4% of all cancer occurrences among women, making it the second most common type of non-skin cancer (after lung cancer) and the fifth most common reason of cancer death [5, 7].

In 2004, breast cancer instigated 519,000 deaths globally (7% of cancer deaths; almost 1% of all deaths). Breast cancer is about 100 times more common in women than in men, while males tend to have poorer outcomes due to postponements in diagnosis. Cancer cells are very similar to cells of the organism from which they developed and have similar (but not identical) DNA and RNA. This is the reason why they are not very commonly recognized by the immune system, in particular, if it is weakened [6, 7].

BSA is most rich protein in blood plasma. It shows high accumulation in inflamed and cancerous place in the body [8]. It has long blood circulating half-life of 19 days and many binding sites [9]. Bovine serum albumin is a serum albumin protein derived from cows. It is frequently used as a protein concentration standard. Lycoat RS 720 is synthetic polymer of pea starch. It

shows good solution stability and film forming property. It is the sustained and controlled release polymer [10]. Betulinic acid is used as a new auspicious agent to treat the Breast cancer [11]. Betulinic acid has been designated as a novel cytotoxic compound active against breast cancer cells [12]. Induction of apoptosis by BA involved mitochondrial perturbations, since inhibition of the mitochondrial permeability transition by the mitochondrion-specific inhibitor bongkreikic acid condensed BA encouraged apoptosis [11, 12]. In addition, mitochondria undergoing BA induced permeability transition triggered DNA fragmentation in isolated nuclei [13]. Cytochrome c was free from mitochondria of BA treated cells, and might be involved in activation of caspases [14]. Following treatment with BA, caspase-8, caspase-3 and PARP were proteolytically processed. Inhibition of caspase cleavage by the broad-range caspase inhibitor zVAD.fmk strongly reduced BA induced apoptosis [13, 14 and 15]. Betulinic acid shows poor bioavailability and poor solubility.

The aim of this research study to develop BA loaded polymeric nanoparticles for active delivery through intravenous route for treatment of breast cancer. Betulinic acid used as a model anti-cancer agent loaded in the conjugated nanoparticles by solvent evaporation method. The nanoparticles were then characterized for their size and size distribution, surface morphology, drug encapsulation efficiency, drug loading and drug release profile. Additional, nanoparticles were tested in vitro for anticancer cell line study.

2.MATERIALS AND METHOD

2.1. Materials

The drug of choice in the present investigation, Betulinic acid was obtained from Aktin Chemicals (Chengdu, China) as gift sample. Bovine Serum Albumin (Fraction V) was obtained from HiMedia Pvt. Ltd., Mumbai, India, as gift sample. Lycoat RS 720 was procured from Roquette Pharma Pvt. Ltd, Mumbai, India. Methanol, acetonitrile of HPLC grade was purchased from Merck Pvt. Ltd, Mumbai, India. All other chemicals were of analytical grade and all chemicals were used as received.

2.2. Method

2.2.1. Drug -Excipients Interaction Study

FTIR spectra of Betulinic acid, BSA, Lycoat RS 720, and physical mixture of polymer with betulinic acid were studied. Above samples were mixed with KBr of IR grade in the ratio of 1:100 and compressed by motorized pellet press at 10-12 tones pressure. The pellets were then scanned using FTIR spectrophotometer (8400S Shimadzu, Japan) within range 4000-400 cm^{-1} . The FTIR spectra of mixtures were compared with that of the FTIR Spectra of pure drug and polymer, to confirm any changes occur or not in the principle peaks of spectra of plain drug and polymer [16].

3.FORMULATION AND DEVELOPMENT

3.1. formulation of bsa-lycoat rs 720 conjugates

These Conjugates were prepared by Maillard reaction. BSA and Lycoat RS 720 were liquefied together in water with a (1:1) molar ratio. The pH of the solution was adjusted to 7.1 with NaOH solution, then, the mixture solution was lyophilized. The lyophilized powder reacted at 60°C and 79% relative humidity in a desiccator containing saturated KBr solution for 24 h. The resultant products were kept at -20°C before use [9, 17].

3.2. characterization of bsa-lycoat rs 720 conjugates ftir spectroscopy

The chemical structure of conjugates was confirmed with Fourier Transform Infrared Spectroscopy (FTIR) before use. FTIR spectra of Bovine serum albumin, Lycoat RS 720 and BSA-LYCOAT RS 720 were studied. Above samples were mixed with KBr of IR grade in the ratio of 1:100 and compressed by motorized pellet press at 10-12 tones pressure. The pellets were then scanned using FTIR spectrophotometer (8400S Shimadzu, Japan) within range 4000-400 cm^{-1} . The FTIR spectra of BSA-LYCOAT RS 720 were compared with separate of the FTIR Spectra of bovine serum albumin and Lycoat RS 720 to confirm the conjugation [16].

3.3. uv-visible absorption spectroscopy

The amount BSA conjugated with Lycoat RS 720 was assessed using the UV absorption spectroscopy technology. BSA-LYCOAT RS 720 (10 mg) was dissolved in water (100 mL). Then, the solution was scanned in the range of 200 nm to 400 nm by UV-spectrophotometer

(UV 1700, Shimadzu, Japan). Degree of conjugation of BSA on a weight basis was calculated by using the following equation: Conjugation of BSA (wt %) = Weight of BSA in conjugate/Total weight of conjugate ×100 [16].

3.4. differential scanning calorimetry (dsc)

DSC Thermogram of BSA, Lycoat RS 720 and BSA-LYCOAT RS 720 was related using DSC (Mettler DSC 1 star system, Mettler-Toledo, Switzerland) at a heating rate of 10°C/min. The measurements were performed at a heating range of 30 to 250°C under nitrogen atmospheres [20].

3.5. x-ray diffractometry (xrd)

The powder X-ray diffraction (Bruker AXS D8 Advance) patterns of BSA, Lycoat RS 720 and BSA-LYCOAT RS 720 were conducted using X-ray diffractometer with Cu as a target at a voltage of 40 kV. Samples were analyzed in 2θ angle range of 10–50° at a scanning rate of 3°/2θ/min [16].

3.6. formulation of polymeric nanoparticles

Polymeric nanoparticles were prepared by the solvent evaporation technique. The polymeric nanoparticles were prepared by using different drug to polymer conjugates ratio (1:1, 1:2 and 1:4). Betulinic acid was dissolved in methanol and conjugates dissolved in 5 ml of water. The mixture was then subjected to Rotary evaporator (KNF LABS RC 600, Switzerland) for removal of the methanol. The dispersion is formed. It was subjected to high speed homogenizer (10,000 RPM for 15 min) and then passed through high pressure homogenizer at pressure of 700 bars and 7 cycles. Nanoparticles solution subjected to lyophilization and dry lyophilized powder of nanoparticles was formed [9, 17].

3.7. formulation design

Different batches of Betulinic acid loaded polymeric nanoparticles were prepared based on the 3² factorial designs. The independent variables were Polymer conjugates concentration in terms of mg (X₁) and HPH

pressure in terms of bar (X₂) with the drug concentration of 10 mg for all formulation batches [17].

3.8. optimization data analysis and model-validation

ANOVA was used to establish the statistical validation of the polynomial equations generated by Design Expert® Software. Fitting a multiple linear regression model to a 3² Factorial design give a predictor equation incorporating interactive and polynomial term to evaluate the responses:

$$Y = b_0 + b_1X_1 + b_2X_2 + b_{12}X_1X_2 + b_{11}X_1^2 + b_{22}X_2^2 \text{----- (1)}$$

Where Y is the measured response associated with each factor level combination; b₀ is an intercept representing the arithmetic average of all quantitative outcomes of nine runs; b_i (b₁, b₂, b₁₁, b₁₂ and b₂₂) are regression coefficients computed from the observed experimental values of Y and X₁ and X₂ are the coded levels of independent variables. The terms X₁ X₂ represent the interaction terms.

Three dimensional response surface plots resulting from equations were obtained by the Design Expert® software.

4.CHARACTERIZATION OF POLYMERIC NANOPARTICLES

4.1. particle size, zeta potential and pdi analysis

The particle size and PDI was measured using dynamic light scattering. Dynamic light scattering (also known as PCS- Photon Correlation Spectroscopy) measures Brownian motion and tells this to the size of the particles. It does this by enlightening the particles with a laser and analyzing the intensity fluctuations in the scattered light. All samples were diluted with double distilled water to yield a appropriate scattering intensity. The zeta potential and PDI values were obtained at an angle of 90° using disposable polystyrene cells having 10 mm diameter at 25°C. Zeta potential was measured by determining the electrophoretic mobility. The average particle size, zeta potential of the nanoparticles was calculated for optimized batch by using Zetasizer (Nano ZS90, Malvern ltd., UK) [16, 18 and 19]. (n = 6).

4.2. entrapment efficiency and drug loading

Nanoparticles dispersion was centrifuge (Bachman Coulter USA) at 12,000 rpm for 2 hrs, 1.0 mL of the supernatant composed after centrifugation was diluted with phosphate buffer pH7.4 and then makes up volume up to 10 ml in 10ml volumetric flask and measured by HPLC at 210 nm. The entrapment efficiency of the nanoparticles was calculated for each batch of nanoparticles [16, 18]. The entrapment efficiency (EE %) and drug-loading (DL %) of betulinic acid in polymeric nanoparticles was calculated from the following equation:

$$\% EE = \frac{\text{amount of drug added} - \text{amount of drug in supernatant}}{\text{amount of drug added}} \times 100 \text{----- (1)}$$

$$\% DL = \frac{\text{Weight of Drug in Nanoparticles}}{\text{Weight of Nanoparticles}} \times 100 \text{----- (2)}$$

4.3. production yield

The production yield of nanoparticles of numerous formulation were calculated using the weight of final product after drying with respect to the initial total weight of the drug and polymer conjugates used for preparation of polymeric nanoparticles [20].

$$\text{Production yield} = \frac{\text{Amount of freezed dried powder}}{\text{Amount of Drug and Polymer in feed}} \times 100 \text{----- (3)}$$

4.4. surface morphological study

Surface morphology of the BA-NP was performed by using transmission electron microscopy (Jeol/JEM 2100). A BA-NP (1 mg/ml) was located on Formvars coated copper grids and permitted to equilibrate. Excess liquid was removed with a filter paper and dried at room temperature for about half an hour. The dried grid containing the BA-NP was visualized using TEM [16, 21 and 22].

4.5. differential scanning calorimetry study

Differential scanning Calorimetry of pure drug and optimized drug loaded polymeric nanoparticles were conducted using differential scanning calorimeter

(Mettler DSC 1 star system, Mettler-Toledo, Switzerland) at heating rate of 10 °C/min over a temperature range of 40 to 350 °C under an inert atmosphere flushed with nitrogen at a rate of 20 mL/min [16].

4.6. determination of drug content by hplc

Betulinic acid was assayed by HPLC (Agilent Technologies, 1200 series) employing a 4.5 × 250 mm C-18 m Qualisil column according to a validated method stated in previous studies with some modifications. The analysis was performed using a solution of Acetonitrile and Water (70:30) as mobile phase in a flow rate of 1 mL/min, using PDA detector at 210 nm. The system was calibrated using standard solutions of BA over the range of 10-50 µg/mL with (R²= 0.9912) [23].

4.7. in-vitro drug release

In vitro diffusion study of lyophilised powder of optimised batch was carried out by Franz diffusion cell (Electro lab, Mumbai) having 2.0 cm diameter and 12.5 ml capacity. Dialysis membrane (HiMedia) having molecular weight cut off range 12000 – 14000 kDa was used as diffusion membrane. Pieces of dialysis membrane were soaked in phosphate buffer pH 7.4 for 24 h prior to experiment. Diffusion cell was filled with saline phosphate buffer, pH 7.4 and dialysis membrane was mounted on cell. The temperature was maintained at 37°C ± 0.5°C. After a pre-incubation time of 20 minutes, the lyophilised powder equivalent to 10 mg of BA was dispersed in 10 ml of saline phosphate buffer pH 7.4 and was placed in the donor chamber. Samples were periodically withdrawn from the receptor compartment for 24 hours having 1, 2, 4, 6, 12, 24 hours of time interval and replaced with the same amount of fresh phosphate buffer and assayed by HPLC at 210 nm [16, 24 and 25].

4.8. model fitting to drug release profile

To study the release kinetics of optimized formulation, data obtained from *in- vitro* drug release studies were plotted in various kinetic models. Zero order as cumulative amount of drug released Vs time, first order as log cumulative percentage of drug remaining vs. time, and Higuchi's model as cumulative percentage of drug released vs. square root of time [26].

4.9. mechanism of drug release

To evaluate the mechanism of drug release from BA loaded polymeric nanoparticles, data for the drug release was plotted in Korsmeyer-Peppas equation as log cumulative percentage of drug released vs. log time. The release exponent n and K value was calculated through the slope of the straight line [26].

4.10. in-vitro anticancer activity

Activity was under processed.

4.11. accelerated stability study

An accelerated stability study was carried out for optimized lyophilized BA-loaded polymeric nanoparticles according to ICH Q1A (R2) guidelines. The stability study was performed at $25 \pm 2^\circ\text{C}/60 \pm 5\% \text{RH}$ in an environmental stability chamber over a period of 180 days to assess the stability of BA-loaded polymeric nanoparticles. The dried powder was transferred to amber-colored glass vials, which were plugged, sealed and kept in the stability chamber. These dried powder samples were redispersed in double distilled water. The MPS, PDI and Zeta potential were measured up to three months [27].

5.RESULTS AND DISCUSSION

5.1. Drug -Excipient Interaction Study

The possible chemical interaction of drug with excipients was seen by drug excipient compatibility carried out for a period of 3 weeks. At the end of three weeks physical mixture of excipient with drug were analyzed by IR spectroscopy. IR spectra of physical mixture and pure drug were shown in figure 1 (A) and (B). Wave numbers of principle peaks observed in the IR spectrum of pure BA are present in the FTIR spectra of physical mixture 3506.70 OH-stretching 2939.61 CH-stretching 1687.77 C=O stretching, 1456.30 C-H bending etc. Thus, it confirms compatibility between drug and polymer and shows no interaction [16].

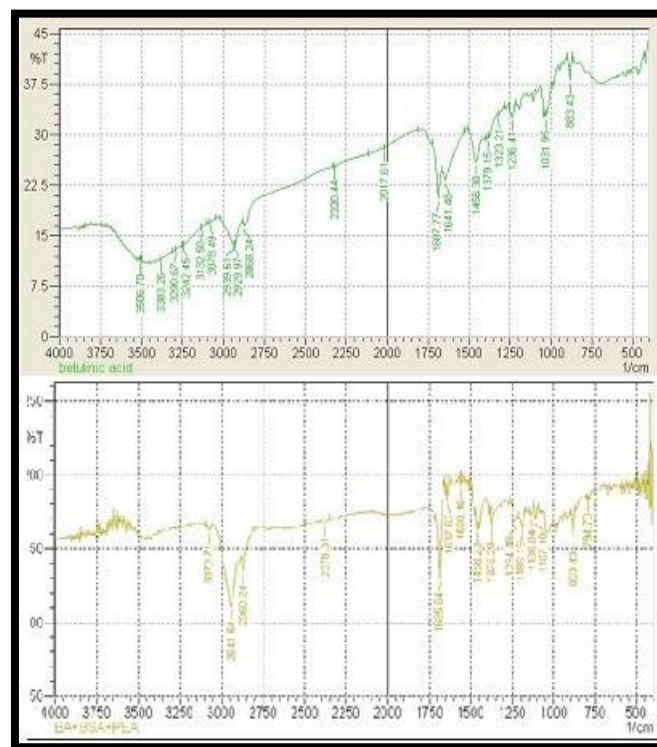


Figure No 1 (A) IR spectrum of BA and (B) spectrum of physical mixture

5.2. Characterization of BSA-LYCOAT RS 720 Conjugates

5.2.1. FTIR Spectroscopy

IR spectra of polymer and protein were shown in figure 2 (A) and (B). Both polymer and protein show same functional group in conjugates spectra as compare with individual polymer spectra except at wave number 1656 cm^{-1} showed (CO-NH). OH stretching at wave number 3446.91 cm^{-1} show intense broad peak in IR spectra of conjugates. Hence, we were concluding that conjugation was done [16].

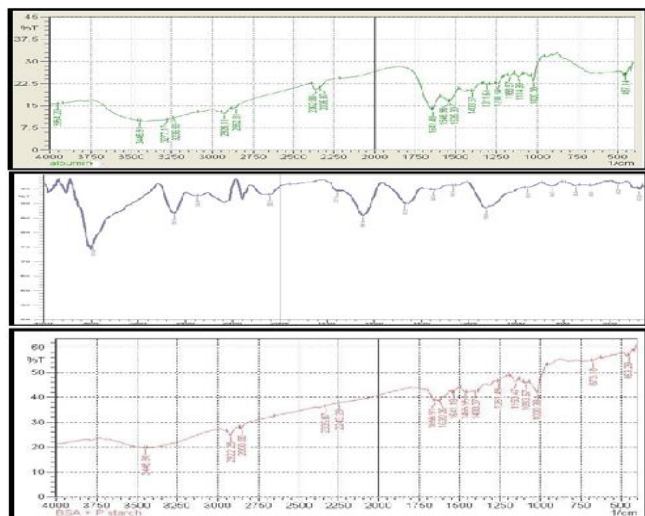


Figure No 2 (A) IR spectrum of BSA and (B) IR spectrum of Lycoat RS 720 (C) IR spectrum of Conjugates

5.3. UV-Visible absorption Spectroscopy

Preliminary determination of conjugates was acquired using UV-Visible spectra in which LYCOAT RS 720 does not show any absorbance peaks from 200 to 400 nm. BSA showed its characteristic peaks at 206 nm and 278 nm. In conjugates, the characteristic UV absorbance peaks around 278 nm appeared in the spectra indicating the presence of BSA in the conjugate. Degree of conjugation of BSA onto LYCOAT RS 720 was found to be 2.69% [16].

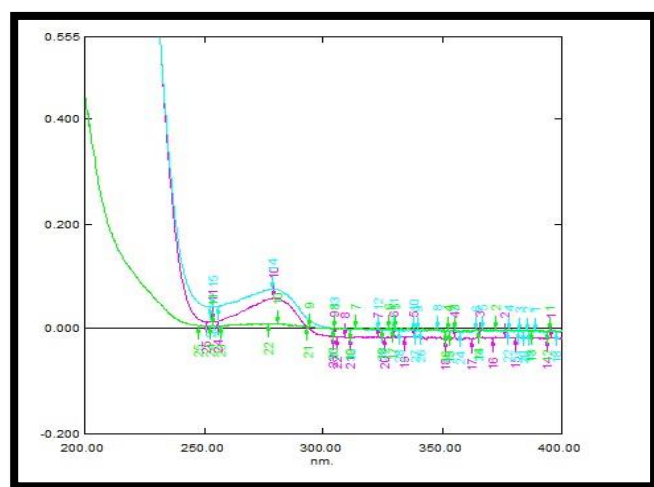


Figure No 3: UV-Absorption spectra of BSA-LYCOAT RS 720

5.4. Differential Scanning Calorimetry (DSC)

DSC Thermogram of BSA and LYCOAT RS 720 showed sharp endothermic peak at 31.54° C and 77.18° C respectively, indicating crystalline nature. However, the both BSA and LYCOAT RS 720 peaks were disappeared in the conjugate with appearance of new peaks at 156.36° C indicating compound BSA-LYCOAT RS 720 conjugate [21].

5.5. X-Ray Diffractometry (XRD)

BSA-LYCOAT RS 720 conjugates showed partly amorphous structure as observed from powder X-ray diffraction pattern. The diffractogram of BSA showed characteristics diffraction peaks at 2θ values of 7.368°, 12.280°, and 19.342° indicating crystalline nature. LYCOAT RS 720 showed blunt diffraction peaks at 9.671° and 20.339° indicating amorphous nature. BSA-LYCOAT RS 720 conjugates showed different diffraction peaks of Lycoat RS 720 at 2θ values of 9.62° and 20.418° with less intensity and intensity of BSA peaks decreased instantly showed amorphous nature [16, 21].

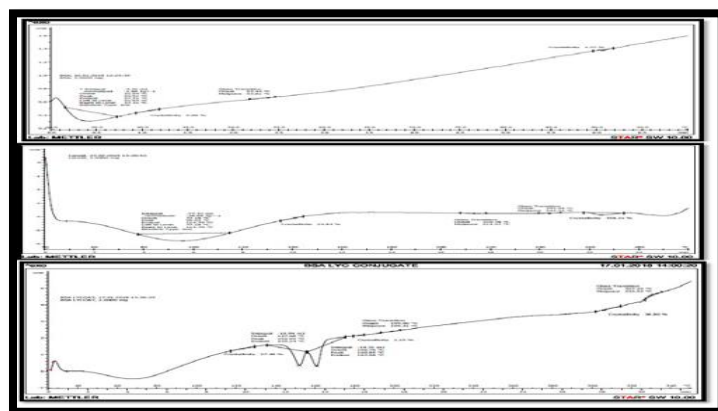


Figure No 4: (A) DSC Thermogram of BSA and (B) DSC Thermogram of Lycoat RS 720 (C) DSC Thermogram of Conjugates

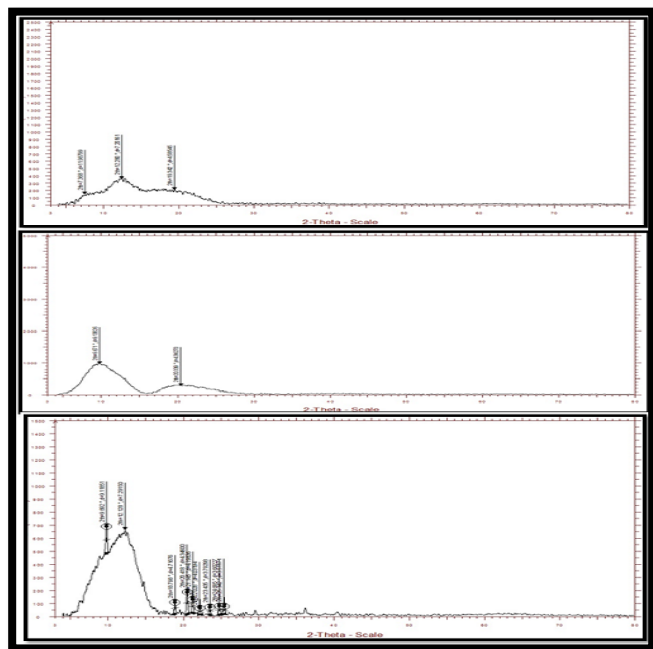


Figure No 5: (A) XRD Pattern of BSA (B) XRD Pattern of Lycoat RS 720 (C) XRD pattern of Conjugates Formulation Design:

Various Formulation batches of Polymeric nanoparticles were prepared based on 3^2 factorial designs. The independent variables were Polymer conjugates concentration in terms of mg (X_1) and HPH pressure in terms of bar (X_2) and their levels are shown in table 1 MPS i.e. Mean Particle Size (d.nm) (Y_1) and Entrapment Efficiency (%) (Y_2), were taken as response parameters as the dependent variables [17].

Table No.1: Formulation Design Batches

Formulation Code	X1 (mg)	X2 (Bar)	Y1 (d.nm)	Y2 (%)
F1	10	800	430	80.5
F2	10	800	450	80.9
F3	40	500	329	86.6
F4	40	300	377	87
F5	20	500	343	85.32
F6	20	500	257	88.32
F7	10	300	390	87.32
F8	20	800	456	80
F9	40	500	325	87

5.6. Optimization data analysis and model-validation

5.6.1. Fitting of data to model

Dependent variables demonstrate that the model was significant for all the response variables. It was observed that independent variables X_1 (Polymer Concentration) and X_2 (HPH Pressure) had a positive effect on the entrapment efficiency and a desired particle size of nano-formulation that is nanoparticles was achieved. The statistical evaluation was performed by using ANNOVA. Results are shown in table 2. The coefficients with more than one factor term in the regression equation represent interaction terms. It also shows that the relationship between factors and responses is not always linear. When more than one factor are changes simultaneously and used at different levels in a formulation, a factor can produce different degrees of responses.

Table No.2: Results of Analysis of Variance for Measured Response

Source of Variation	Sum of Square	D F	Mean of Square	F Value	p-value Prob > F	Summary Significant
Model (MPS)	30891.33	4	7722.83	7.58	0.0376	Significant
X1-Polymer Conc. (mg)	813.50	2	406.75	0.40	0.6950	
X2-HPH Press. (bar)	3963.00	2	1981.50	1.94	0.02571	
Source of Variation	Sum of Square	D F	Mean of Square	F Value	p-value Prob > F	Summary Significant
Model (EE)	83.68	4	20.92	16.78	0.0091	Significant

X1- Polym ar Conc. (mg)	0.052	2	0.026	0.02 1	0.979 6	
X2- HPH Press. (bar)	35.25	2	17.63	14.1 4	0.015 4	

5.7. 3D Surface Plot Analysis

Three dimensional surface plots were generated by the Design Expert® software are presented in (Fig.6 (A) and Fig.6 (B)) for the studied responses, i.e. Mean Particle Size (Y1) and Entrapment Efficiency (Y2). Fig.6 (A) depicts response surface plot of Polymer Conjugate Concentration (X1) and HPH Pressure (X2) on Mean Particle Size. Nanoparticles being nanoparticulated structures, formulation batch amongst all the design batches giving least particle size will be preferred more and selected as an optimized batch. Where F6 Design Batch, with a polymer concentration of about 20 mg and HPH pressure 500 bar, shows the least particle size i.e. 257 nm. Fig.6 (B) depicts response surface plot of Polymer Conjugate Concentration (X1) and HPH Pressure (X2) on entrapment efficiency. The 3-D surface image shows a linear response, which indicates with the increase in the polymer concentration the entrapment efficiency increases, as more the polymer available more will be the entrapment efficiency.

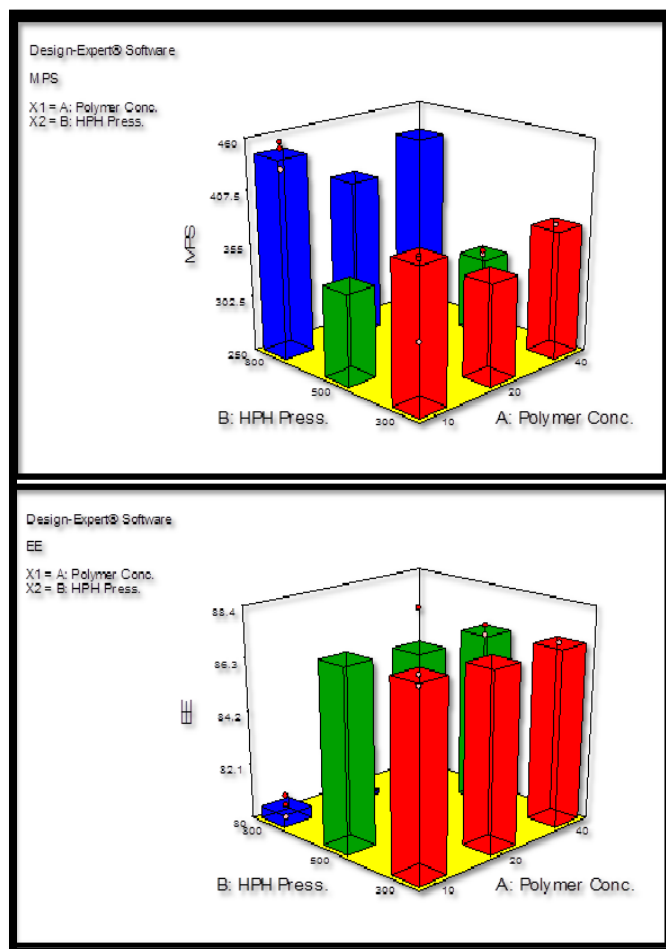


Figure No 6: (A) 3D surface plots for X1 and X2 on Mean Particle Size (Y1), where X1= Polymer Conjugates Concentration and X2= HPH Pressure (B) 3D surface plots for X1 and X2 on Entrapment Efficiency (Y1), where X1= Polymer Conjugates Concentration and X2= HPH Pressure

Here two design batches i.e. F6 and F7 show maximum entrapment efficiency i.e. 88.32% and 87.32% respectively. But as seen in first response Surface graph being a nanoparticle formulation considering the least particle size is also a crucial factor. So, the Design Batch with least particle size and maximum entrapment efficiency is selected. Therefore, F6 is considered as an optimised Batch [17].

6.CHARACTERIZATION OF POLYMERIC NANOPARTICLES

6.1. Particle Size and Particle size distribution study

The particle size of the PNs is a fundamental factor because it decides the rate and extent of drug release as well as drug absorption. The smaller particle size offers a larger interfacial surface area for drug absorption and improves the bioavailability. The calculation of polydispersity index takes into account the particle mean size, the refractive index of the solvent, the measurement angle and the variance of the distribution. Low polydispersity index value might be associated with a high homogeneity in the particle population, whereas high polydispersity index values suggest a broad size distribution or even several populations. The optimized formulation batch (F6) showed mean particle size 310 nm before lyophilization while 257 nm after lyophilization with PDI 0.589 and 0.533 respectively. The MPS and PDI were decreased in freeze-dried powder. This might be due to adherence of cryoprotectant throughout freeze-drying. The optimization of cryoprotectant was based on appearance of cake and ease of reconstitution [16, 18 and 19].

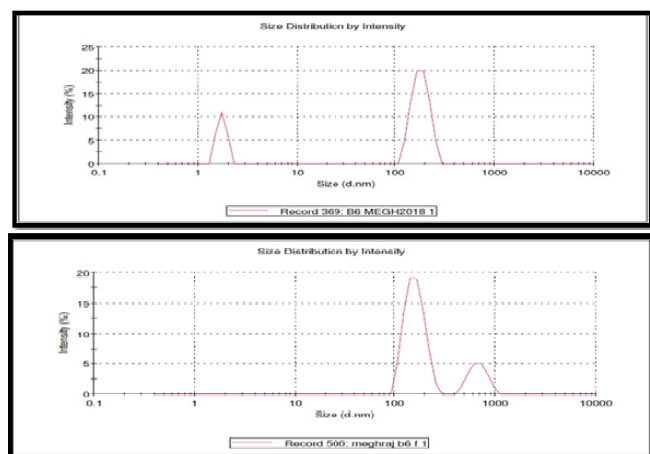


Figure No 7: (A) Particle size of Formulation Batch before Lyophilization (F6) (B) Particle size of Formulation Batch after Lyophilization (F6) Zeta Potential Measurement

The zeta potential values of plain drug, blank nanoparticles and drug loaded nanoparticles that was found to be -10.2 mV, -30.9 mV and -22.4 mV respectively [18, 19].

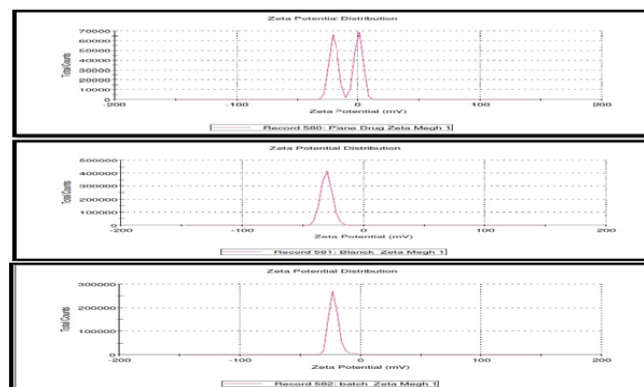


Figure No 8: (A) Zeta Potential of Plane Drug (B) Blank Nanoparticles (C) Formulation Batch Entrapment efficiency and Drug Loading

The % EE of optimized batch was found to be 88.32 ± 0.61 . The % DL was found to be 6.84 ± 0.52 . It has been reported that, increase in the polymer conjugates concentration the entrapment efficiency increases, as more the polymer available more will be the entrapment efficiency [16, 18].

6.2. Production Yield

All the batches showed production yield in between 86-96%. The resultant yield is an indication that the method can be appropriate for technology transfer that is production on large scale. The optimized batch showed production yield was found to be 95.66 ± 0.24 [20].

6.3. Surface Morphological Study

Surface morphology of the Polymeric Nanoparticles was evaluated using transmission electron microscope (TEM) from which it can be seen that the nanoparticles have smooth surfaces. Nanoparticles show spherical shape with size 200 nm [16, 21 and 22].

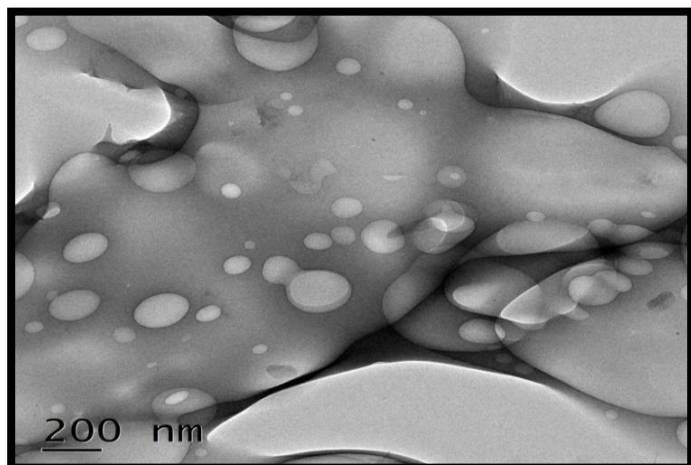


Figure No 9: TEM Image of Formulation Batch (F6)
 Differential scanning Calorimetry (DSC):

In case of formulation (F6) no peak was observed in the range of 313.41 °C which confirms the molecular dispersion of the drug in the polymer matrix and entrapment inside the polymeric nanoparticles (Figure 10). Peak present in range 157-164°C show the presence of mannitol in the given formulation [16].

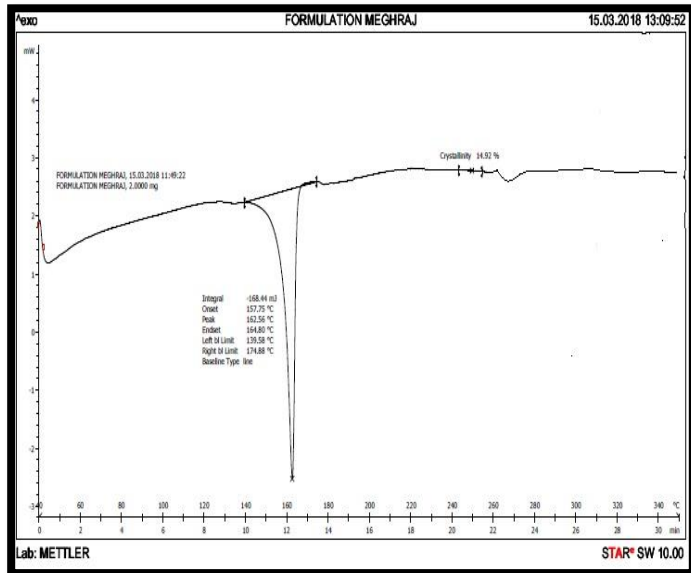


Figure No 10: DSC of Formulation Batch (F6)
 Drug Content by HPLC

The optimized batch F6 shows drug content of 78.10%. From the below chromatogram it was revealed that, the retention time of BA was found to be 13.4 min [23].

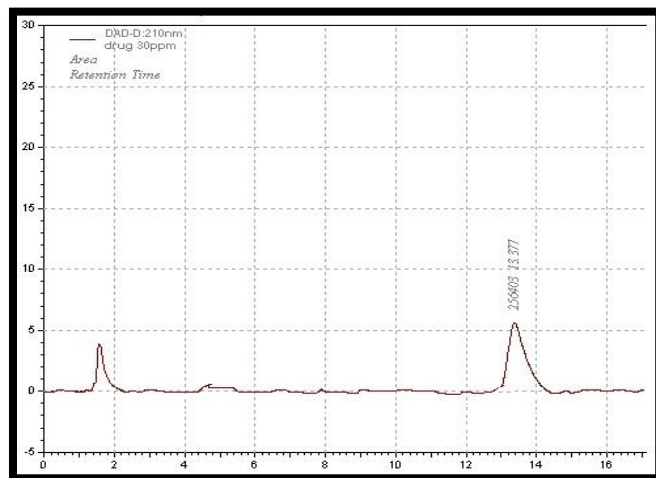


Figure No 11: Chromatogram of Optimized Batch (F6)

6.4. *In vitro* Drug Release

In vitro drug release was carried out for nanoparticles. Fig.12 shows comparison drug release between nanoparticles and pure drug suspension. The drug is release study is being carried out by means of using diffusion cell apparatus. The release of drug from polymeric nanoparticles depends upon the nature of polymer. Formulation nanoparticles showed similar release patterns differing only slightly in terms of burst and cumulative drug release with pure suspension. The release of free BA was found to be rapid and reached 100% cumulative within 12 hrs. In case of nanoparticles, an initial burst release was observed for first 6 hrs (45-65%), after which release of BA from nanoparticles increased steadily up to 24 hrs. A burst drug release was observed in the beginning, which may be due to the smaller particle size that attributed to the large surface area of the nanoparticles, apart from it diffusion of the drug from the outer shell of the nanoparticles may be responsible for initial burst release. Nanoparticles were compared with pure drug solution which tells that, incorporation of drug in polymeric nanoparticles gives Controlled release. Polymeric nanoparticles showed considerable enhanced release pattern for a period of about 24 hrs. The % Diffusion value after carrying out the entire *in-vitro* study was found to be 94.24±0.33% [16, 24 and 25].

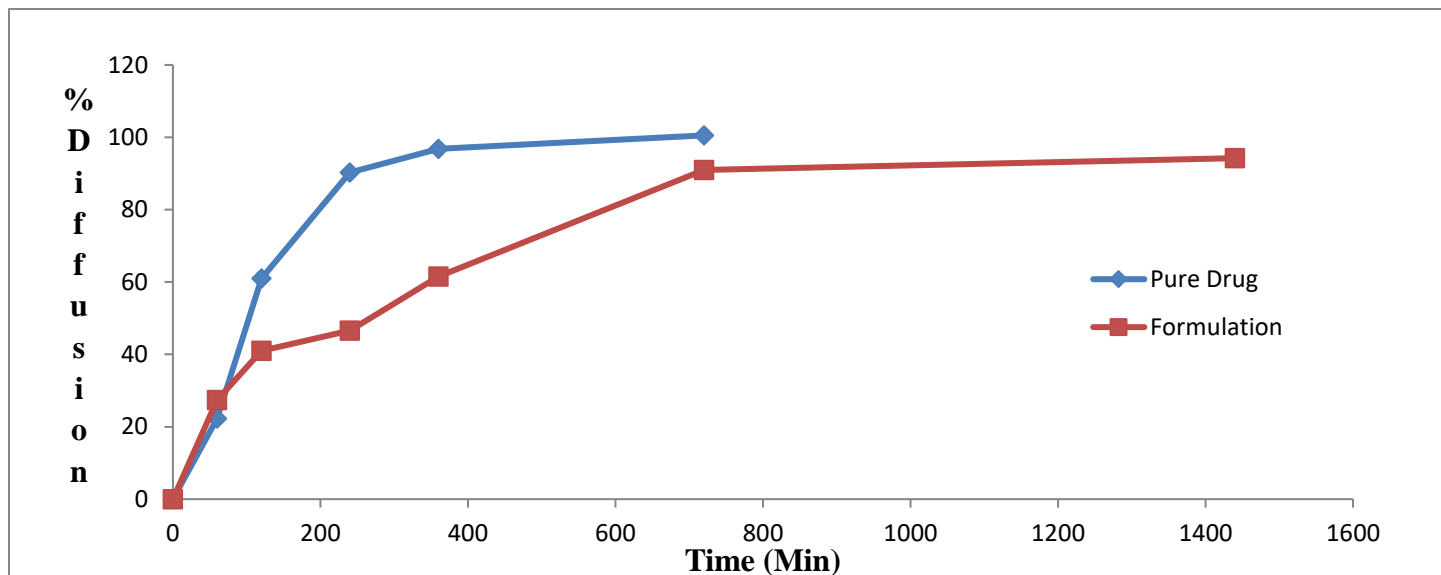


Figure No 12: In vitro drug release of BA-Suspension and optimized BA-Nanoparticle

6.5. Mechanism of drug release

The corresponding plot of (log cumulative percent drug release Vs log time) of the Korsmeyer-Peppas equation indicated a good linearity of regression coefficient (R²) 0.9646. The release exponent (n) of Korsmeyer-Peppas equation was found to be 0.6468 and K value 0.1237 [26].

6.6. In-Vitro Anticancer Activity

Samples were submitted for analysis and result waited.

6.7. Accelerated Stability Study

Accelerated stability studies of formulation were conducted by measurement of particle size, PDI and zeta potential. Before stability studies, BA loaded PNPs showed mean particle size 257±0.47 nm with PDI 0.533±0.46. After stability studies mean particle size and PDI was found to be 261±0.12 nm and 0.539±0.21 respectively. There were no significant changes in particle size and PDI after three month storage. Zeta potential of optimized formulation before and after stability study was found to be -22.4±15 mV and -22.2±0.19 mV, respectively. Based on these results it is revealed that, BA loaded PNPs (Formulation batch F6) was found to be stable formulation at the given temperature and humidity condition [27].

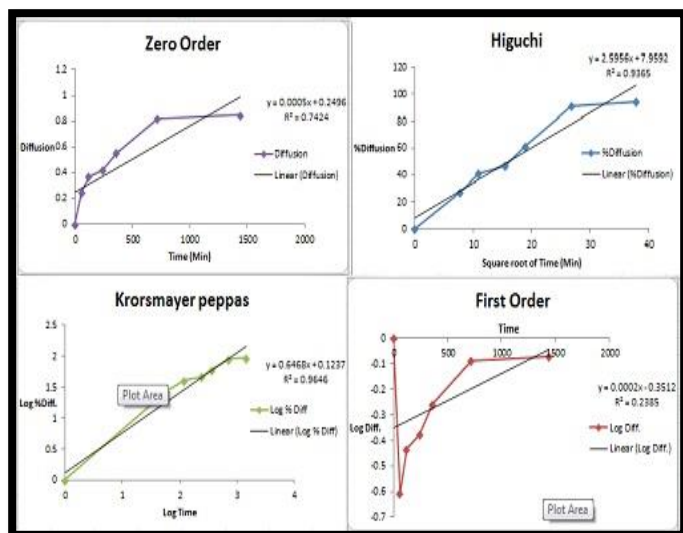


Figure No 13: Release Kinetics of Nanoparticles

7.CONCLUSION

Betulinic Acid loaded polymeric nanoparticles have been developed successfully to minimize processing variables in the manufacturing process. The batch optimization

was done on the basis of lower particle size, zeta potential, drug content and desired drug release in desired manner. The drug loaded polymeric nanoparticles can be demonstrated as a potential carrier to improve solubility of BA. Polymeric nanoparticles are unique drug delivery system which can be administered by intravenous route and thus it can be used in controlled and targeted drug delivery.

8.ACKNOWLEDGMENT

Authors are thankful to Aktin Chemicals, Chengdu, China for providing gift sample of betulinic acid. The authors are also thankful HiMedia Pvt. Ltd. Mumbai, India, for providing gift sample of BSA. The authors are also thankful Roquette Pharma Pvt. Ltd, Mumbai, India, for providing gift sample of Lycoat RS 720. The authors are also grateful to Principal (R. C. Patel Institute of Pharmaceutical Education and Research, Shirpur) for providing necessary facilities and infrastructure for carrying out this work.

REFERENCES

- [1] Nikam, A.P., Mukesh, P.R. and Haudhary, S.P., 2014. Nanoparticles—an overview. *J. Drug Deliv. Ther*, 3, pp.1121-1127.
- [2] Jawahar, N. and Meyyanathan, S.N., 2012. Polymeric nanoparticles for drug delivery and targeting: A comprehensive review. *International Journal of Health & Allied Sciences*, 1(4), pp.217-223.
- [3] Abhilash, M., 2010. Potential applications of Nanoparticles. *Int J Pharm Bio Sci* 1(1), pp. 7-9.
- [4] Nagavarma, B.V.N., Yadav, H.K., Ayaz, A., Vasudha, L.S. and Shivakumar, H.G., 2012. Different techniques for preparation of polymeric nanoparticles-a review. *Asian J. Pharm. Clin. Res*, 5(3), pp.16-23.
- [5] Sharma, G.N., Dave, R., Sanadya, J., Sharma, P. and Sharma, K.K., 2010. Various types and management of breast cancer: an overview. *Journal of advanced pharmaceutical technology & research*, 1(2), pp.109-115.
- [6] Osborne, C., Wilson, P. and Tripathy, D., 2004. Oncogenes and tumor suppressor genes in breast cancer: potential diagnostic and therapeutic applications. *The oncologist*, 9(4), pp.361-377.
- [7] Ingvarsson, S., 2001, October. Breast cancer: introduction. In seminars in CANCER BIOLOGY (Vol. 11, No. 5, pp. 323-326). Academic Press.
- [8] Smith, A.A., Zuwala, K., Pilgram, O., Johansen, K.S., Tolstrup, M., Dagnæs-Hansen, F. and Zelikin, A.N., 2016. Albumin–polymer–drug conjugates: long circulating, high payload drug delivery vehicles. *ACS Macro Letters*, 5(10), pp.1089-1094.
- [9] Edelman, R., Assaraf, Y.G., Levitzky, I., Shahar, T. and Livney, Y.D., 2017. Hyaluronic acid-serum albumin conjugate-based nanoparticles for targeted cancer therapy. *Oncotarget*, 8(15), pp.24337-24353.
- [10] Ratnayake, W.S., Hoover, R. and Warkentin, T., 2002. Pea starch: composition, structure and properties—a review. *Starch-Stärke*, 54(6), pp.217-234.
- [11] Yogeewari, P. and Sriram, D., 2005. Betulinic acid and its derivatives: a review on their biological properties. *Current medicinal chemistry*, 12(6), pp.657-666.
- [12] Evan, G. I.; Vousden, K. H. 2001. Proliferation, cell cycle and apoptosis in cancer. *Nature* 411, pp.342-348.
- [13] Pisha, E., Chai, H., Lee, I.S., Chagwedera, T.E., Farnsworth, N.R., Cordell, G.A., Beecher, C.W., Fong, H.H., Kinghorn, A.D., Brown, D.M. and Wani, M.C., 1995. Discovery of betulinic acid as a selective inhibitor of human melanoma that functions by induction of apoptosis. *Nature medicine*, 1(10), pp.1046-1051.
- [14] Fulda, S.; Scaffidi, C.; Susin, S. A.; Krammer, P. H.; Kroemer, G.; Peter, M. E.; Debatin, K. M. 1998. Activation of mitochondria and release of mitochondrial apoptogenic factors by betulinic acid. *J. Biol. Chem.* 273, pp. 33942-33948.
- [15] Fulda, S.; Susin, S. A.; Kroemer, G.; Debatin, K. M. 1998. Molecular ordering of apoptosis induced by anticancer drugs in neuroblastoma cells. *Cancer Res.* 58, pp. 4453-4460.
- [16] Pawar, A., Singh, S., Rajalakshmi, S., Shaikh, K. and Bothiraja, C., 2018. Development of fisetin-loaded folate functionalized pluronic micelles for breast cancer targeting. *Artificial cells, nanomedicine, and biotechnology*, pp.1-15.
- [17] Cavazzuti, M., 2013. Design of experiments. In *Optimization Methods* (pp. 13-42). Springer Berlin Heidelberg.
- [18] Qi, J., Yao, P., He, F., Yu, C. and Huang, C., 2010. Nanoparticles with dextran/chitosan shell and BSA/chitosan core—doxorubicin loading and delivery.

International journal of pharmaceutics, 393(1-2), pp.177-185.

[19] Zhao, L., Du, J., Duan, Y., Zhang, H., Yang, C., Cao, F. and Zhai, G., 2012. Curcumin loaded mixed micelles composed of Pluronic P123 and F68: preparation, optimization and in vitro characterization. *Colloids and Surfaces B: Biointerfaces*, 97, pp.101-108.

[20] Mahajan, H.S. and Mahajan, P.R., 2016. Development of grafted xyloglucan micelles for pulmonary delivery of curcumin: in vitro and in vivo studies. *International journal of biological macromolecules*, 82, pp.621-627.

[21] Bothiraja, C., Rajput, N., Poudel, I., Rajalakshmi, S., Panda, B. and Pawar, A., 2018. Development of novel biofunctionalized chitosan decorated nanocochleates as a cancer targeted drug delivery platform. *Artificial cells, nanomedicine, and biotechnology*, pp.1-15.

[22] Bronze-Uhle, E.S., Costa, B.C., Ximenes, V.F. and Lisboa-Filho, P.N., 2017. Synthetic nanoparticles of bovine serum albumin with entrapped salicylic acid. *Nanotechnology, science and applications*, 10, pp.11-21.

[23] Taralkar, S.V. and Chattopadhyay, S., 2012. A HPLC Method for determination of ursolic acid and betulinic acids from their methanolic extracts of *Vitex Negundo* Linn. *Journal of analytical and bioanalytical Techniques*, 3(3), pp.1-6.

[24] Madane, R.G. and Mahajan, H.S., 2016. Curcumin-loaded nanostructured lipid carriers (NLCs) for nasal administration: design, characterization, and *in vivo* study. *Drug delivery*, 23(4), pp.1326-1334.

[25] Sahib, M.N., Abdulameer, S.A., Darwis, Y., Peh, K.K. and Tan, Y.T.F., 2012. Solubilization of beclomethasone dipropionate in sterically stabilized phospholipid nanomicelles (SSMs): physicochemical and *in vitro* evaluations. *Drug design, development and therapy*, 6, pp.29-42.

[26] Costa, P. and Lobo, J.M.S., 2001. Modeling and comparison of dissolution profiles. *European journal of pharmaceutical sciences*, 13(2), pp.123-133.

[27] Jain, S., Mittal, A., K Jain, A., R Mahajan, R. and Singh, D., 2010. Cyclosporin A loaded PLGA nanoparticle: preparation, optimization, and in-vitro characterization and stability studies. *Current Nanoscience*, 6(4), pp.422-431.